Rectifying Behavior in Coulomb Blockades: Charging Rectifiers

M. Stopa

Tarucha Mesoscopic Correlation Project, ERATO-JST, 4S-308S, NTT Atsugi Research and Development Laboratories, 3-1 Morinosato-Wakamiya, Atsugi-shi Kanagawa-ken, 243-0198 Japan

(Received 25 April 2001; published 25 March 2002)

We introduce examples of tunneling and diffusive, Coulomb-regulated rectifiers based on the Coulomb blockade formalism in discrete and continuum systems, respectively. Nonlinearity of the interacting dynamics profoundly enhances the inherent asymmetry of the devices by reducing the Hilbert space of accessible states. The discrete charging rectifier is structurally similar to hybrid molecular electronic rectifiers, while the continuum-charging rectifier is based on a model of ionic flow through a pore (ion channel) with an artificial branch. The devices are formally related to ratchet systems with spatial periodicity replaced by a winding number: the current.

DOI: 10.1103/PhysRevLett.88.146802 PACS numbers: 73.40.Ei, 73.23.Hk, 85.35.Gv, 87.16.Uv

Ratchets typically involve diffusive or driven motion of *noninteracting* particles in a potential whose principal feature is its lack of inversion symmetry [1]. This chirality, typified by the "sawtooth" potential, extracts energy from colored noise or an unbiased driving force and thereby imparts directed motion to the particles of the system. In certain biochemical contexts [2], a similar "chiral dynamics" is seen in the directed motion of a discrete reaction coordinate, typically governed by a rate equation. The quantum Brownian problem in a sawtooth potential [3], when driven beyond the linear regime, has also been reduced to an effective discrete rate problem, with the rates determined via tunneling path integrals in the semiclassical limit, and the system was shown to exhibit thermally reversible rectification.

Besides the reaction coordinate formalism, which includes interaction only implicitly, interparticle interactions in ratchet systems have been treated by site-exclusion models [4], nearest-neighbor spring constant interactions [5], Kuramoto-type interactions [6], and finite size, hard-core repulsion studies [7]. The recently developed Coulomb blockade formalism, however, also expresses (incoherent) transitions between *many-body* states of quantum dots, clusters and arrays in terms of a master equation [8], with the states specified by the numbers of electrons, n_i, on the collection of dots (in addition to voltages on gates and leads). Further, the investigation of rectifying effects in the mesoscopic regime, where it is known that these charging effects can dominate transport, has become recently very active [9,10]. Therefore it is natural to examine systems where single charge, Coulomb interaction physics produces the parameter-dependent asymmetry of rate matrices that are the hallmark of ratchet and other rectifying mechanisms.

In Figure 1 we introduce as an archetype a triple-dot Coulomb blockade rectifier. This structure can be readily realized in a two-dimensional electron gas (2DEG) heterostructure. Interaction is conveniently introduced by a capacitance matrix, and transport proceeds according to the usual single electron tunneling formalism [8]. We illustrate a portion of the "stability diagram" for three dots, with zero source-drain bias, in Fig. 1(C). A quadruple point exists where the states with a single excess electron on each dot, denoted $|1\rangle$, $|2\rangle$, and $|3\rangle$, and the zero electron state $|0\rangle$ are all mutually degenerate. The gates adjacent to the dots can be tuned to this quadruple point, in

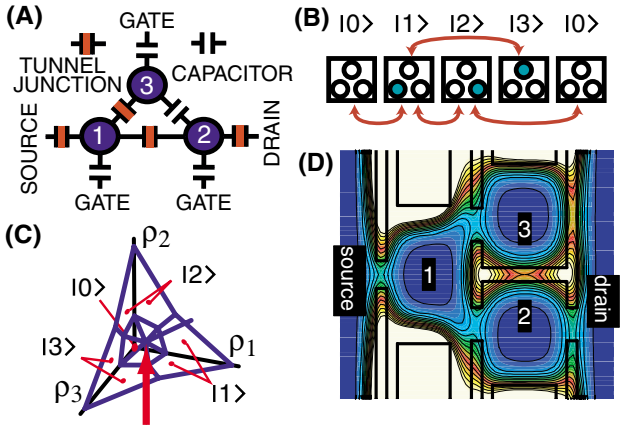

FIG. 1 (color). (A) Schematic of triple-dot rectifier. Tunnel junctions (red blocks) are leaky capacitors allowing quantum mechanical, single electron tunneling. Dots 2 and 3 *capacitively* interact, but tunneling is forbidden, making the structure asymmetric. External gates coupled to dots allow adjustment of stable electron configuration, assuming zero source-drain bias. (B) Illustration of connectivity between states in triple-dot rectifier. Notation for states defined in text. In the forward-bias condition state $|3\rangle$ is a trap since the rate γ_{31} exceeds γ_{13} exponentially. (C) Stability diagram for the triple-dot showing the vertex where states $|0\rangle$, $|1\rangle$, $|2\rangle$, and $|3\rangle$ are degenerate (red arrow). ρ_i is the induced charge on dot i proportional to the voltage on the gate adjacent to i. (D) Potential contour from the self-consistent electronic structure calculation for GaAs-AlGaAs 2DEG heterostructure with the model triple-dot rectifier surface gate pattern. The dot centers are at ~ -10 meV, saddle points of barriers at ~ 14 meV. All capacitances employed in I-V calculations (Fig. 2) are determined from this model. Capacitances between dots and leads can be adjusted by modulating the gates controlling the "quantum point contact" openings (gaps in the gates).

a fashion similar to the operating principle of the double-dot electron pump [11]. For sufficiently low temperatures the Coulomb interaction prohibits any other states of the system. Specifically, two electrons can never be simultaneously in the array. Chirality is introduced [Fig. 1(A)] by placing an infinite tunnel barrier between dots 2 and 3, even though they continue to interact *capacitively*. In the restricted Hilbert space of these four states the evolution of the state of the system is described by a master equation $\dot{\mathbf{W}} = \mathbf{\Gamma}(V)\mathbf{W}$, where $\mathbf{W}$ is the vector of the four occupation probabilities and the *off-diagonal* elements of the transition matrix $\mathbf{\Gamma}(V)$ are, via the "global rule" [8,12], $\gamma_{ij} = \Delta\mathcal{F}_{ij}/\{e^2R_t[\exp(\beta\Delta\mathcal{F}_{ij}) - 1]\}$ with $i, j = 0, 1, 2, 3$. The isolation of dot 3 from all but dot 1 implies that $\gamma_{03} = \gamma_{23} = \gamma_{30} = \gamma_{32} = 0$. Diagonal elements of $\mathbf{\Gamma}(V)$ are minus the sum of off-diagonal elements in the same column. The global free energy of the system is $\mathcal{F} = A_{nm}q_n(\frac{1}{2}q_m - \rho_m) - \Delta_I V_I$ (summation convention assumed) and $\Delta\mathcal{F}_{ij}$ is the change in this energy due to the transition from *state* j to *state* i. Here q_m is the excess charge on *dot* m, ρ_m is the gate-induced charge on m, and matrix A_{nm} is the inverse of the capacitance submatrix which connects only the dots (i.e., not the leads or gates) [13]. Also, V_I are the lead voltages ($I = 1, 2$) and Δ_I represents the total charge transferred from lead I into the array; the inverse temperature is $\beta = 1/k_BT$ and the tunnel resistance between dots is R_t.

The steady state solution for the probability of occupying state $|1\rangle$ is determined to be [14]

$$W_1 = \left[1 + \frac{\gamma_{31}}{\gamma_{13}} + \frac{\gamma_{01}(\gamma_{20} + \gamma_{02} + \gamma_{12}) + \gamma_{21}(\gamma_{10} + \gamma_{20} + \gamma_{02})}{\gamma_{10}(\gamma_{02} + \gamma_{12}) + \gamma_{20}\gamma_{12}}\right]^{-1}. \quad (1)$$

Also, we find $W_2 = W_1[\gamma_{10}\gamma_{21} + \gamma_{20}(\gamma_{01} + \gamma_{21})]/[\gamma_{20}\gamma_{12} + \gamma_{10}(\gamma_{02} + \gamma_{12})]$, and the current is given simply by $I(V) = \gamma_{21}W_1 - \gamma_{12}W_2$, where $V \equiv V_2 - V_1$.

Recently Linke *et al.* [9] considered the rectifying behavior of a triangular cavity in a 2DEG channel which, beyond the linear source-drain regime, introduced asymmetry into the T matrix for transmission through the system. This arrow-shaped experimental device resembles a weak "herringbone ratchet," as introduced by Cecchi and Magnasco [15] (see below). The purely quantum mechanical, one-body scattering effects would lead to rectification for our device as well, even without charging effects included (i.e., treating the triple dot as a fixed potential scatterer to independent electrons). However, when the charging energy is comparable to or greater than the temperature, $e^2/C \gtrsim k_BT$ (C is a typical capacitance), *interaction becomes dominant* and, as we have seen, the Hilbert space of the system is reduced so that, at most, one excess electron can be in the triple-dot system.

The result is the following. Near $V = 0$ the current is still symmetric, $I(V) = -I(-V)$ [see upper inset of Fig. 2], due to the assumed degeneracy of the levels. For finite bias, capacitive coupling between leads and dots breaks this degeneracy. A forward source-drain bias lowers the energy of $|3\rangle$ relative to $|1\rangle$ and an electron which enters dot 3 (i) becomes trapped and (ii) prevents other electrons from entering the first dot. This is effectively a jamming process [16]. Bias-dependent asymmetry in the matrix Γ is ultimately responsible for breaking the current-voltage symmetry leading, at low T, to "negative resistance" [15]. We can define the "trapping ratio" as the rate into dot 3 divided by the rate out $(\gamma_{31}/\gamma_{13}) = \exp(\beta\Delta\mathcal{F}_{13})$. $\Delta\mathcal{F}_{13}$ depends linearly on the source voltage V_1 and is modulated by the capacitance between the source and the various dots. This implies that tunneling *out* of the "jamming dot" is favored when the bias is reversed. Note that the effect is similar to that in a hybrid molecular electronic (HME) rectifier [17]. The principle of HME rectifiers is based on specific natural configurations, for certain molecules, of the HOMO and LUMO in space and is not normally considered to be a product of electron-electron interaction. In

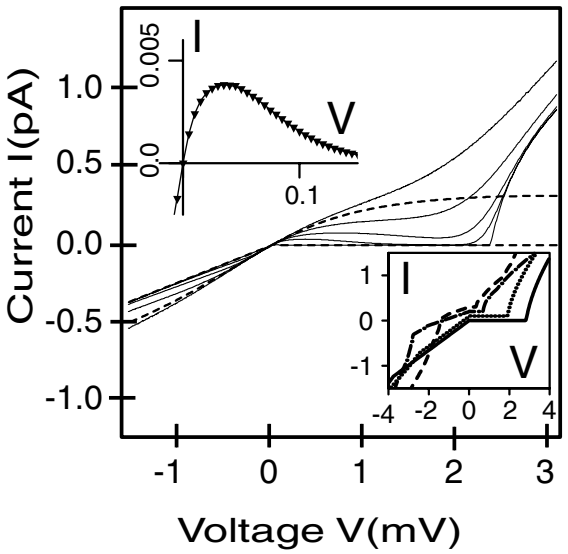

FIG. 2. I-V characteristic for a triple-dot rectifier. The current in the forward-bias ($V > 0$) direction is strongly blocked by electron trapping in dot 3; $C = 0.083$ fF, $C_{dd} = 0.025$ fF. The dashed lines are from the master equation with $T = 0.05$ K (lower curve for $V > 0$) and 4.0 K. The solid lines, $T = 0.05$, 0.5, 1.0, 2.0, and 4.0 K (from bottom for $V > 0$), are full Monte Carlo simulations. Deviation occurs when voltage induces multiple charge states in the device. The trend with T is reversed for $V < 0$ (i.e., lines cross at $V = 0$). Upper inset: closeup of low voltage region for $T = 0.05$ K; the line is the master equation, and the triangles are Monte Carlo. Lower inset: I-V (Monte Carlo) for $C = 0.056$ fF, $C_{dd}/C = 1/3.3$ (solid line); $C = 0.083$ fF, $C_{dd}/C = 1/3.3$ (dotted line); $C = 0.083$ fF, $C_{dd}/C = 1/5$ (dash-dotted line); $C = 0.167$ fF, $C_{dd}/C = 1/5$ (dashed line). All $T = 0.05$ K. The top three curves offset vertically by 0.05, 0.1, and 0.15 pA for clarity.

our case the specific allowed states depend critically on the many-body state and not merely the static properties of the individual quantum dots themselves.

Rectification in discretized ratchet models [3] also arises from parameter-dependent asymmetry in the rate matrix. The rate equation is often truncated to model a single period of the potential, and a winding number, which in our case is the source-drain current, counts the particles transferred from one period to the next.

Full 3D simulations of the electronic structure of a prototype, GaAs-AlGaAs rectifier, Fig. 1(D), provide typical capacitance values. These simulations [18] are effective mass, local density approximation solutions of the electronic structure, including the GaAs wafer profile, gate geometries and voltages, donor density, and wide lead regions, carried out within density functional theory. The particular results shown here have further assumed the density in the 2DEG x-y plane to be separable from that in z and given by the 2D Thomas-Fermi approximation.

With the 2DEG layer positioned 140 nm below the surface, with a donor layer of density 3.1×10^{11} cm^{-2} at 20 nm above the GaAs-AlGaAs interface, quantum dots of radius $r \sim 200$ nm are formed, each containing roughly 150 electrons. The self-capacitance of one dot is $C \approx 5 \times 10^{-17}$ F with a charging energy $e^2/C \approx 3$ meV. Interdot capacitances vary with barrier thicknesses; typically $C_{dd} \approx 0.8 \times 10^{-17}$ F, or roughly 15% of the self-capacitance. Using these capacitances, the free energy differences in Γ can be computed. The current given by the steady state solution to the master equation, Eq. (1), is shown in Fig. 2. We also show full Monte Carlo (MC) simulations of the transport through this structure [12,19], where the Hilbert space *is not* restricted to only four states. The linearity near $V = 0$ and the jamming of the current at larger biases are evident in both results; however, for sufficiently large bias, the MC simulation shows that the current again increases. In this case the bias is sufficient to move the system away from the quadruple point and other, multiple electron, charge states become accessible, i.e., the blocking is overcome.

Quantum mechanical tunneling is generally irrelevant in biological systems, where ratchet science finds some of its most profound applications. Nonetheless, the correlating effect of single charge interaction can be significant even in continuum systems characterized by drift and diffusion. In a recently developed model for ionic flow in biological ion channels, the capacitance model of Coulomb blockade physics was used for a 1D approximation of the electrostatic interaction of the ions in a background dielectric medium (i.e., water) [20]. A continuum limit of the capacitance array model can be taken and the resulting equation is equivalent to a drift-diffusion treatment of *interacting* particles. The Brownian dynamics of ion flow through a pore, including a Langevin force, ion diffusivities, and short-range ion-ion repulsion (added "by hand"), were thereby simulated self-consistently. The computation time for the simulation is reduced significantly in comparison to models which solve a full 3D Poisson equation at each time step [21]. Furthermore, in contrast to self-consistent drift-diffusion studies, which have remarkable success modeling the I-V characteristics of realistic ion channels [22], the discrete nature of the ion charge is included in the model, allowing for treatment of noise properties and single charge correlation effects.

Here, we employ an *ion-channel–like* system and demonstrate that single charging phenomena can induce rectification in a continuum system. We *artificially* add an asymmetric branch to an ion channel, Fig. 3(A). Asymmetry is manifested in the model by a finite capacitance between the end of the branch and one of the leads. Aside from the branch, which has no particular biological

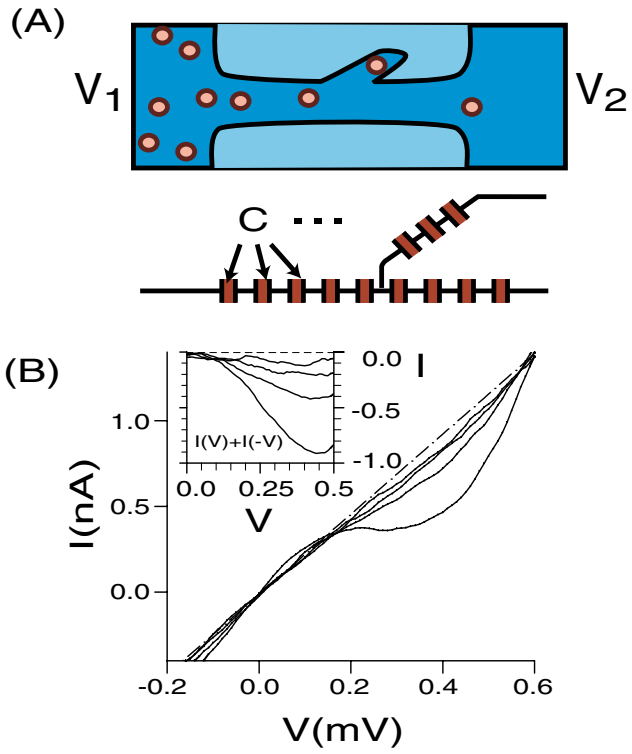

FIG. 3 (color). (A) Schematic for the branching channel rectifier. Based on biological ion channel structure, a tube filled with a dielectric medium (water), isolated ions execute Brownian motion between electrochemical baths at fixed potentials V_1 and $V_2 = -V_1$. The main channel length is 3 nm, branch length 0.5 nm, and channel and branch radii 0.15 nm. The total interacting energy computed at each time step of the Monte Carlo simulation employing an approximation of 1D capacitance array, modeled to fit the actual interaction of charges in a dielectric-filled cylinder, $\kappa_{H_2O} = 80$, surrounded by a medium with $\kappa_{\text{protein}} = 2$ (see Ref. [20]). (B) I-V characteristics from MC simulations at (from the bottom at $V = 0.3$ mV) $T = 150$, 200, 250, and 300 K employing 0.75, 1.5, 3, and 6×10^6 time steps, respectively. The top (dash-dotted line) line is the linear extrapolation of $V < 0$ I-V for $T = 300$ K. The parameters for the sodium ion are employed, including mass $m_{\text{Na}} = 3.8 \times 10^{-23}$ g, radius $r_{\text{Na}} = 0.095$ nm, and diffusion coefficient $D_{\text{Na}} = 1.3 \times 10^{-5}$ cm^2 s^{-1} (see Ref. [21]). The inset is the current added to its mirror image same order of curves as above, showing rectification even at room temperature (top dashed line is zero).

motivation [23], the electrostatic and transport parameters are taken from the structure of a typical ion channel (using Na as the diffusing ion) [21], see Fig. 3. A typical value of the capacitance length which approximates the Coulomb interaction of a pair of point charges along the central axis of a dielectric-filled tube with dielectric constant $\kappa_{H_2O} = 80$ surrounded by a "protein" with $\kappa_{\text{protein}} = 2$ is $C \sim 8 \times 10^{-20}$ Fnm. A capacitance to ground must also be included but, for these parameters, is very small.

As in the triple-dot model, ions which diffuse into the upper branch are drawn toward the drain in forward bias and, while trapped there, inhibit subsequent ions from approaching the branch junction. In reverse bias the ions vacate the branch, and flow is uninhibited. The Coulomb interaction between two ions at opposite ends of the channel is approximately 15 meV or about 170 K. We find that even at $T = 300$ K the repulsion between individual charges is sufficient to induce a noticeable asymmetry into the I-V characteristic, Fig. 3(B). The asymmetry is even more pronounced for lower, albeit nonphysical, temperatures. Thus a "device" of the form of Fig. 3(A), in the presence of a rocking potential or colored noise, would pump ions in the reverse-bias direction.

Note that this structure is similar in configuration to the model studied in Ref. [15]. The principal difference is that, with interparticle interaction, the trapping of a single ion in a crevice in the channel serves to inhibit the flow of other ions.

Interaction reduces the accessible phase space for a system of flowing particles. Depending on the asymmetry built into the system, this can lead to a blockade or jamming of current in one direction while leaving flow uninhibited in the other direction. We have discussed only two possible realizations of rectifying behavior resulting primarily from particle-particle interaction as treated within the capacitance matrix formalism of the Coulomb blockade, but many other examples can be formulated. As a final example, a spin-blockade mechanism in asymmetric, serially coupled quantum dots has recently been proposed for a diode whose phase space blocking results from a combination of charging and Pauli exclusion effects [24], resulting in what might be called a Coulomb spin-blockade rectifier.

The author thanks H. Linke, P. Hänggi, and R. Eisenberg for helpful conversations.

[1] For a recent review, see P. Reimann, Phys. Rep. **361**, 57 (2002).
[2] R. D. Astumian, J. Phys. Chem. **100**, 19 075 (1996).
[3] P. Reimann, M. Grifoni, and P. Hänggi, Phys. Rev. Lett. **79**, 10 (1997).
[4] K. W. Kehr and Z. Koza, Phys. Rev. E **61**, 2319 (2000) [see also included references on "totally asymmetric site-exclusion process" (TASEP)].
[5] F. Marchesoni, Phys. Rev. Lett. **77**, 2364 (1996).
[6] R. Hänssler, R. Bartussek, and P. Hänggi, in *Applied Nonlinear Dynamics and Stochastic Systems Near the Millenium,* edited by J. B. Kadtke and A. Bulsara, AIP Conf. Proc. No. 411 (AIP, New York, 1997).
[7] I. Derényi and T. Vicsek, Phys. Rev. Lett. **75**, 374 (1995). One additional interesting work which treats an interacting ratchet system, but is somewhat difficult to classify otherwise, is B. Cleuren and C. van den Broeck, Europhys. Lett. **54**, 1 (2001).
[8] *Single Charge Tunneling,* edited by H. Grabert and M. H. Devoret (Plenum, New York, 1992).
[9] H. Linke *et al.,* Science **286**, 2314 (1999).
[10] A. M. Song *et al.,* Phys. Rev. Lett. **80**, 3831 (1998).
[11] H. Pothier *et al.,* Europhys. Lett. **17**, 249 (1992).
[12] U. Geigenmüller and G. Schön, Europhys. Lett. **10**, 765 (1989); M. Stopa, Phys. Rev. B **64**, 193315 (2001).
[13] M. Stopa, Y. Aoyagi, and T. Sugano, Phys. Rev. B **51**, 5494 (1995).
[14] H. Risken, *The Fokker-Planck Equation* (Springer-Verlag, Berlin, 1989); N. G. van Kampen, in *Advances in Chemical Physics,* edited by I. Prigogine and S. A. Rice (Wiley, New York, 1976), Vol. XXXIV, pp. 245–309.
[15] G. A. Cecchi and M. Magnasco, Phys. Rev. Lett. **76**, 1968 (1996).
[16] C. S. O'Hern *et al.,* Phys. Rev. Lett. **86**, 111 (2001).
[17] A. Aviram and M. Ratner, Chem. Phys. Lett. **29**, 277 (1974); C. Joachim, J. K. Gimzewski, and A. Aviram, Nature (London) **408**, 541 (2000); A. Nitzan, Annu. Rev. Phys. Chem. **52**, 23 (2001).
[18] M. Stopa, Phys. Rev. B **54**, 13 767 (1996); Semicond. Sci. Technol. **13**, A55 (1998); Physica (Amsterdam) **251B**, 228 (1998).
[19] P. Delsing, T. Claeson, K. K. Likharev, and L. S. Kuzmin, Phys. Rev. B **42**, 7439 (1990).
[20] M. Stopa, Superlattices Microstruct. **27**, 617 (2000); M. Stopa, Phys. Rev. B **64**, 193315 (2001).
[21] S-H. Chung *et al.,* Biophys. J. **75**, 793 (1998).
[22] W. Nonner and R. Eisenberg, Biophys. J. **75**, 1287 (1998); D. Chen, J. Lear, and R. Eisenberg, Biophys. J. **72**, 97 (1997).
[23] Note, however, the concluding discussion and references in Ref. [15].
[24] K. Ono *et al.* (unpublished).